DERIVATION AND VALIDATION OF A SPATIAL MULTI–LINK HUMAN POSTURAL STABILITY MODEL

Nicholas R. Bourgeois[1], Robert G. Langlois[1]
[1]*Department of Mechanical and Aerospace Engineering, Carleton University, Ottawa, Canada*
Email: Nicholas.Bourgeois@carleton.ca; Robert.Langlois@carleton.ca

ABSTRACT

In naval engineering and related disciplines, it is common for dynamic models of the human body to be used in conjunction with quantitative records of body and ship motions, in order to study human balance behaviour while performing various shipboard activities. Research in this area can lead to improvements in ship operations and designs that improve crew safety and efficiency. This paper presents the development of a new spatial 18 degree-of-freedom (DOF) ship-inverted pendulum model that incorporates 6 DOF ship motion and 3 DOF joints representing ankle, knee, waist, and neck motions. The derived model is then validated by comparing it to similar models derived using alternative methods but simulated under equivalent input conditions.

Keywords: Kane's method; human postural stability; inverted pendulum.

DÉRIVATION ET VALIDATION D'UN MODÈLE DE STABILITÉ POSTURALE HUMAIN SPATIALE AVEC DE MULTIPLES LIENS

RÉSUMÉ

Mots-clés : .

1. INTRODUCTION

Dynamic models of the human body can be used to study human postural response to moving environments. Presented here is the development and validation of a multi-link spatial model intended to be used to study the relationship between sensory inputs and human balance performance. The procedure used to derive the model is novel because it uses a method of automatically deriving the equations of motion in three dimensions in a format which can be directly written in the standard matrix form of $\mathbf{Ax} = \mathbf{b}$ without additional algebraic manipulation. Validation of the model is accomplished by comparing simulation results with three published models of varying complexity.

2. MOTIVATION

It is generally agreed upon that multibody dynamics modelling techniques are well suited to problems in biomechanics and nonlinear system design [1]. In particular, the chain-link structure of the human body makes it well suited to being modelled with multibody dynamics derivation methods that are capable of automatically generating and solving the equations of motion of mechanical systems, if the mass properties, geometrical properties, connection types, and externally applied forces of the system are known beforehand [2]. Many postural stability models with four or more links have been derived in two dimensions; however, few exist in three dimensions due to the computational complexity. Some models have been developed that combine separate sagittal and frontal plane models [3, 4]. A spatial inverted pendulum model has been developed for use in shipboard research [5] and a double-link spatial inverted pendulum has been developed for use in studying balance control in robots [6].

Typically the number of links in an inverted pendulum postural stability model is defined by the specific types of motion that one wishes to study. As far back as 1981, it was identified that a single-link inverted pendulum does not adequately describe human postural dynamics, since investigations show that significant movement occurs at all joints, not only at the ankle [7]. An experiment was carried out where the joint angles of subjects were monitored after experiencing translational displacements and there was significant movement measured at ankle, knee, waist, and neck joints. This indicated that a model with at least four degrees of freedom in two dimensions was necessary to represent human sway. Additional research has shown that a model with at least four links is needed for studying sensory control mechanisms [8], and that neglecting to include a knee joint can greatly limit possible control strategies [9]. There is also evidence that the a human's head position receives additional stabilization control in order to maintain a stable optical image of the world [10, 11]. Less research has been conducted on the usefulness of spatial postural stability models, but those that have point out that centrifugal and Coriolis forces have no equivalent in a planar model due to their formulation as cross products [6], and that correlations with experimental results imply that a three-dimensional model is necessary in order to fully understand how balance is maintained in everyday life [12].

Based on these past studies, the objective of the current work is to derive the equations of motion for a multi-link spatial inverted pendulum for use in studying human postural stability on board ships at sea. A four-link inverted pendulum model was chosen to allow for motion equivalent to that provided by ankles, knees, waist, and neck.

3. SIMULATION CONFIGURATION

The system to be simulated consists of a human standing on the deck of a ship which is operating in a variety of sea states. Figure 1 shows the general structure and sequence of operations for the simulation. This paper will focus mainly on the 'system dynamics model' and 'comparison to other models' components.

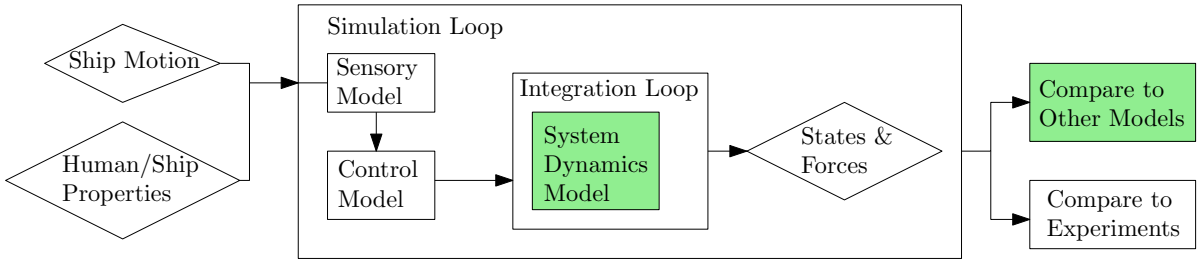

Fig. 1. Overall simulation operations flow.

3.1. System Configuration

The coordinate systems and degrees of freedom defined in the model are shown in Fig. 2. There are 18 degrees of freedom (DOF) divided among the five bodies, which are modelled using generalized coordinates derivatives labelled as $\dot{\mathbf{x}}_i^k$, where k indicates body number, and i is a sequential index for each body. Coordinate system 0 is the origin in inertial space. Coordinate system 1 is the ship body-fixed coordinate system, and is located at the inverted pendulum attachment point. The X-axis points toward the ship bow (front), and Y-axis points toward port (left). Coordinate systems 2 through 5 are body-fixed coordinate systems for each of the four inverted pendulum links.

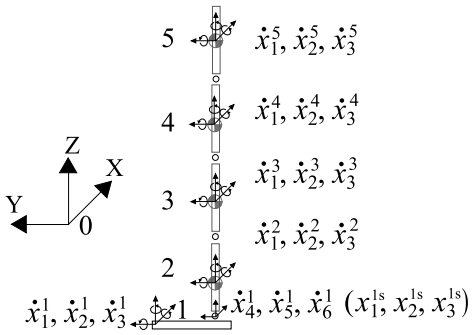

Fig. 2. Model coordinate systems and generalized coordinate derivatives.

The first 6 DOF define the dynamics of the ship's motion. The translational DOF of the ship are defined in the ship frame rather than the inertial frame for reasons that will be discussed subsequently.

4. DERIVATION OF THE EQUATIONS OF MOTION

The derivation of the equations of motion used here is based on an automated method of deriving the equations of motion for open chain-like mechanisms in a form that lends itself well to matrix mathematics [13]. The notations used in [13] have been modified for this paper in order to satisfy standard variable labelling practices. The method presented in [13] also does not go into detail on several important aspects, including how to properly extend the procedure to three degrees of freedom per joint, how to incorporate translational degrees of freedom, and how to solve for reaction forces resulting from constrained motion. In order to accommodate these limitations, a second reference was used which documents a similar automated method of deriving the equations of motion, but in tensor notation [14]. While tensor notation lends itself well to the syntax of programming languages, ensuring that the simulation code is correctly implemented can be more difficult.

4.1. General Equations of Motion

Based on Kane's method and the principle of virtual work [13], Euler's equations of motion of a system can be written as:

$$\sum_{k}\sum_{i} \mathbf{f}^k \frac{\partial \mathbf{v}^k}{\partial q_i} = \sum_{k}\sum_{i} m^k \dot{\mathbf{v}}_G^k \frac{\partial \mathbf{v}^k}{\partial q_i} \tag{1}$$

$$\sum_{k}\sum_{i} \mathbf{m}^k \frac{\partial \mathbf{w}^k}{\partial \dot{x}_i} = \sum_{k}\sum_{i} \left[\mathbf{I}^k \dot{\mathbf{w}}^k + \mathbf{w}^k \times (\mathbf{I}^k \mathbf{w}^k)\right] \frac{\partial \mathbf{w}^k}{\partial \dot{x}_i} \tag{2}$$

The index k is cycled over the number of bodies in the system, and the index i is cycled over the number of generalized speeds, $\mathbf{q}^k$, and generalized coordinate derivatives, $\dot{\mathbf{x}}^k$, defined for each body. The terms $\mathbf{w}^k$

and $\mathbf{v}_G^k$ are the angular velocity and velocity of the centre of gravity, respectively. If the velocity partial derivatives are written as $\mathbf{V}^k$ and $\mathbf{W}^k$, and $\mathbf{Q}$ is the transformation between $\dot{\mathbf{x}}^k$ and $\mathbf{q}^k$, then $\mathbf{v}_G^k$ and $\mathbf{w}^k$ can be written as:

$$\mathbf{v}_G^k = (\mathbf{q}^k)^T \mathbf{V}^k = (\dot{\mathbf{x}}^k)^T \mathbf{Q} \mathbf{V}^k = (\dot{\mathbf{x}}^k)^T \mathbf{V}_Q^k \tag{3}$$

$$\mathbf{w}^k = (\dot{\mathbf{x}}^k)^T \mathbf{W}^k \tag{4}$$

These terms and their time derivatives can be substituted into Eqs. (1) and (2) to give:

$$\sum^k \left[(\mathbf{f}^k)^T (\mathbf{V}_Q^k)^T = m^k (\ddot{\mathbf{x}}^k)^T \mathbf{V}_Q^k (\mathbf{V}_Q^k)^T + m^k (\dot{\mathbf{x}}^k)^T \dot{\mathbf{V}}_Q^k (\mathbf{V}_Q^k)^T \right] \tag{5}$$

$$\sum^k \left[(\mathbf{m}^k)^T (\mathbf{W}^k)^T = (\ddot{\mathbf{x}}^k)^T \mathbf{W}^k (\mathbf{I}^{k0})^T (\mathbf{W}^k)^T + (\dot{\mathbf{x}}^k)^T \dot{\mathbf{W}}^k (\mathbf{I}^{k0})^T (\mathbf{W}^k)^T + (\dot{\mathbf{x}}^k)^T \mathbf{W}^k (\mathbf{I}^{k0})^T (\mathbf{\Omega}^k)^T (\mathbf{W}^k)^T \right] \tag{6}$$

where $\mathbf{\Omega}^k$ is the skew-symmetric matrix of $\mathbf{w}^k$ and the superscript $(^{k0})$ indicates that a variable has been defined in local coordinates and transformed to inertial coordinates. Since each term evaluates to a vector, a transpose operation can be performed allowing Eqs 5 and 6 to be simplified to:

$$\sum^k \left[\mathbf{V}_Q^k \mathbf{f}^k = m^k \mathbf{V}_Q^k (\mathbf{V}_Q^k)^T \ddot{\mathbf{x}}^k + m^k \mathbf{V}_Q^k (\dot{\mathbf{V}}_Q^k)^T \dot{\mathbf{x}}^k \right] \tag{7}$$

$$\sum^k \left[\mathbf{W}^k \mathbf{m}^k = \mathbf{W}^k \mathbf{I}^{k0} (\mathbf{W}^k)^T \ddot{\mathbf{x}}^k + \mathbf{W}^k \mathbf{I}^{k0} (\dot{\mathbf{W}}^k)^T \dot{\mathbf{x}}^k + \mathbf{W}^k \mathbf{\Omega}^k \mathbf{I}^{k0} (\mathbf{W}^k)^T \dot{\mathbf{x}}^k \right] \tag{8}$$

Equations 7 and 8 can be combined since they are written in terms of the same variables and the following similar terms can be collected:

$$\mathbf{A} = \sum^k \left[m^k \mathbf{V}_Q^k (\mathbf{V}_Q^k)^T + \mathbf{W}^k \mathbf{I}^{k0} (\mathbf{W}^k)^T \right] \tag{9}$$

$$\mathbf{B} = \sum^k \left[m^k \mathbf{V}_Q^k (\dot{\mathbf{V}}_Q^k)^T + \mathbf{W}^k \mathbf{I}^{k0} (\dot{\mathbf{W}}^k)^T \right] \tag{10}$$

$$\mathbf{C} = \sum^k \mathbf{W}^k \mathbf{\Omega}^k \mathbf{I}^{k0} (\mathbf{W}^k)^T \tag{11}$$

$$\boldsymbol{f} = \sum^k \mathbf{V}_Q^k \mathbf{f}^k + \sum^k \mathbf{W}^k \mathbf{m}^k \tag{12}$$

The equations of motion can then be simply written as:

$$\mathbf{A}\ddot{\mathbf{x}} + \mathbf{B}\dot{\mathbf{x}} + \mathbf{C}\dot{\mathbf{x}} = \boldsymbol{f} \tag{13}$$

4.2. Partial Velocity and Partial Angular Velocity Matrices

The use of partial velocity matrices is a convenient method for automatically generating dynamics equations, as it allows each individual rigid body's state variables to be defined in the body's local coordinate system, and then be transformed to the global coordinate system when substituted into the governing equations.

4.2.1. Partial Angular Velocity Matrices

The first step for determining the partial angular velocity matrices $\mathbf{W}^k$, is to define the coordinate transformation matrices between body coordinate systems. These transformations can then be combined to determine the transformation between each body coordinate system and the inertial coordinate system. For this model, Bryant angles, $\boldsymbol{\theta}^k$, which use an XYZ body-fixed rotation sequence, were selected. This rotation convention is commonly used in ship-based simulations. Coordinate rotations are calculated for each body coordinate system and then are multiplied together to determine the overall rotation from individual body frames to the inertial frame.

The resulting matrix can be used to transform any vector quantity between coordinate systems. This means that given any vector $\mathbf{r}_L$ defined in a local coordinate system, and $\mathbf{R}^{k0}$, a transformation from the local coordinate system to inertial coordinates, one can calculate the vector in inertial coordinates $\mathbf{r}_G$ as:

$$(\mathbf{r}_G)^T = (\mathbf{r}_L)^T \mathbf{R}^{k0} \tag{14}$$

The partial angular velocity matrix is basically the sequence of rotations needed to rotate an angular dimension from a local coordinate system to the global coordinate system. For angular degrees of freedom this is the local to global transformation matrix, and for translational degrees of freedom it is just a zero matrix since the partial angular velocity derivative for a translational coordinate is zero.

In the ship–inverted pendulum system there are 6 DOF associated with the ship and 12 associated with the inverted pendulum, so the resulting partial angular velocity matrices (with dimensions 18x3) can be defined as:

$$\mathbf{W}^1 = \begin{bmatrix} \mathbf{R}^{10} \\ \mathbf{O} \\ \mathbf{O} \\ \mathbf{O} \\ \mathbf{O} \\ \mathbf{O} \end{bmatrix} \mathbf{W}^{1s} = \begin{bmatrix} \mathbf{O} \\ \mathbf{O} \\ \mathbf{O} \\ \mathbf{O} \\ \mathbf{O} \\ \mathbf{O} \end{bmatrix}$$

$$\mathbf{W}^2 = \begin{bmatrix} \mathbf{R}^{10} \\ \mathbf{O} \\ \mathbf{R}^{20} \\ \mathbf{O} \\ \mathbf{O} \\ \mathbf{O} \end{bmatrix} \mathbf{W}^3 = \begin{bmatrix} \mathbf{R}^{10} \\ \mathbf{O} \\ \mathbf{R}^{20} \\ \mathbf{R}^{30} \\ \mathbf{O} \\ \mathbf{O} \end{bmatrix} \mathbf{W}^4 = \begin{bmatrix} \mathbf{R}^{10} \\ \mathbf{O} \\ \mathbf{R}^{20} \\ \mathbf{R}^{30} \\ \mathbf{R}^{40} \\ \mathbf{O} \end{bmatrix} \mathbf{W}^5 = \begin{bmatrix} \mathbf{R}^{10} \\ \mathbf{O} \\ \mathbf{R}^{20} \\ \mathbf{R}^{30} \\ \mathbf{R}^{40} \\ \mathbf{R}^{50} \end{bmatrix} \tag{15}$$

where $\mathbf{O}$ is a 3x3 zero matrix and the superscript (^{s}) differentiates the ship translational DOF from angular DOF.

4.2.2. Partial Velocity Matrices

The partial velocity matrix $\mathbf{V}^k$ is defined in a similar way to the partial angular velocity matrix, except that the dimensions of the links need to be taken into account. The partial velocity matrices of the ship-inverted pendulum model are:

$$\mathbf{V}^1 = \begin{bmatrix} \mathbf{R}^{01}\mathbf{S}_{r1}\mathbf{R}^{10} \\ \mathbf{O} \\ \mathbf{O} \\ \mathbf{O} \\ \mathbf{O} \\ \mathbf{O} \end{bmatrix} \mathbf{V}^{1s} = \begin{bmatrix} \mathbf{R}^{01}\mathbf{S}_{r1}\mathbf{R}^{10} \\ \mathbf{R}^{10} \\ \mathbf{O} \\ \mathbf{O} \\ \mathbf{O} \\ \mathbf{O} \end{bmatrix} \mathbf{V}^2 = \begin{bmatrix} \mathbf{R}^{01}\mathbf{S}_{q1}\mathbf{R}^{10} \\ \mathbf{R}^{10} \\ \mathbf{R}^{02}\mathbf{S}_{r2}\mathbf{R}^{20} \\ \mathbf{O} \\ \mathbf{O} \\ \mathbf{O} \end{bmatrix}$$

$$\mathbf{V}^3 = \begin{bmatrix} \mathbf{R}^{01}\mathbf{S}_{q1}\mathbf{R}^{10} \\ \mathbf{R}^{10} \\ \mathbf{R}^{02}\mathbf{S}_{q2}\mathbf{R}^{20} \\ \mathbf{R}^{03}\mathbf{S}_{r3}\mathbf{R}^{30} \\ \mathbf{O} \\ \mathbf{O} \end{bmatrix} \mathbf{V}^4 = \begin{bmatrix} \mathbf{R}^{01}\mathbf{S}_{q1}\mathbf{R}^{10} \\ \mathbf{R}^{10} \\ \mathbf{R}^{02}\mathbf{S}_{q2}\mathbf{R}^{20} \\ \mathbf{R}^{03}\mathbf{S}_{q3}\mathbf{R}^{30} \\ \mathbf{R}^{04}\mathbf{S}_{r4}\mathbf{R}^{40} \\ \mathbf{O} \end{bmatrix} \mathbf{V}^5 = \begin{bmatrix} \mathbf{R}^{01}\mathbf{S}_{q1}\mathbf{R}^{10} \\ \mathbf{R}^{10} \\ \mathbf{R}^{02}\mathbf{S}_{q2}\mathbf{R}^{20} \\ \mathbf{R}^{03}\mathbf{S}_{q3}\mathbf{R}^{30} \\ \mathbf{R}^{04}\mathbf{S}_{q4}\mathbf{R}^{40} \\ \mathbf{R}^{05}\mathbf{S}_{r5}\mathbf{R}^{50} \end{bmatrix} \tag{16}$$

where $[\mathbf{S}_{rk}]$ and $[\mathbf{S}_{qk}]$ are skew-symmetric matrices of the vectors that define, in body k local coordinates, the link centres of gravity and subsequent link connection points, respectively.

Next, the partial angular velocity matrix $\mathbf{W}^k$ and partial velocity matrix $\mathbf{V}^k$ are differentiated with respect to time in order to obtain $\dot{\mathbf{W}}^k$ and $\dot{\mathbf{V}}^k$.

The inertia matrices $\mathbf{I}^{k0}$ are obtained by defining the inertia properties for each body $\mathbf{I}^k$ in their local coordinate systems and then rotating them into the global coordinate system using the following transformation:

$$\mathbf{I}^{k0} = \mathbf{R}^{k0}\mathbf{I}^k(\mathbf{R}^{k0})^T \tag{17}$$

Finally, the partial velocities $\mathbf{V}^k$ and partial velocity derivatives $\dot{\mathbf{V}}^k$ are pre-multiplied by $\mathbf{Q}$ to obtain $\mathbf{V}^k_Q$ and $\dot{\mathbf{V}}^k_Q$. This allows the equations defined in terms of $\mathbf{q}$ and $\dot{\mathbf{q}}$ to be written in terms of $\dot{\mathbf{x}}$ and $\ddot{\mathbf{x}}$ with the transformation:

$$(\mathbf{q})^T = (\dot{\mathbf{x}})^T\mathbf{Q} \tag{18}$$

For the ship–inverted pendulum model the matrix is:

$$\mathbf{Q} = \begin{bmatrix} \mathbf{R}^{10} & \mathbf{O} & \mathbf{R}^{10} & \mathbf{R}^{10} & \mathbf{R}^{10} & \mathbf{R}^{10} \\ \mathbf{O} & \mathbf{R}^{10} & \mathbf{O} & \mathbf{O} & \mathbf{O} & \mathbf{O} \\ \mathbf{O} & \mathbf{O} & \mathbf{R}^{20} & \mathbf{R}^{20} & \mathbf{R}^{20} & \mathbf{R}^{20} \\ \mathbf{O} & \mathbf{O} & \mathbf{O} & \mathbf{R}^{30} & \mathbf{R}^{30} & \mathbf{R}^{30} \\ \mathbf{O} & \mathbf{O} & \mathbf{O} & \mathbf{O} & \mathbf{R}^{40} & \mathbf{R}^{40} \\ \mathbf{O} & \mathbf{O} & \mathbf{O} & \mathbf{O} & \mathbf{O} & \mathbf{R}^{50} \end{bmatrix} \tag{19}$$

Now that all of the terms in Eq. (13) have been defined, the following sections will discuss how the equations are customized to specific constraint conditions and numerically solved.

4.3. Prescribed Ship Motion

The model's first 6 DOF are ship angular and translational motions, and thus have already been determined when the simulation starts. This means that Eq. (13) can be rearranged (with $\mathbf{y}$ substituted for $\dot{\mathbf{x}}$) as:

$$\mathbf{A}\dot{\mathbf{y}} = \boldsymbol{f} - \mathbf{B}\mathbf{y} - \mathbf{C}\mathbf{y} = \mathbf{d} \tag{20}$$

and partitioned by degrees of freedom as:

$$\begin{bmatrix} [\mathbf{A}_1] & [\quad \mathbf{A}_2 \quad] \\ [\mathbf{A}_3] & [\quad \mathbf{A}_4 \quad] \end{bmatrix} \begin{Bmatrix} [\dot{\mathbf{y}}_1] \\ [\dot{\mathbf{y}}_2] \end{Bmatrix} = \begin{Bmatrix} [\mathbf{d}_1] \\ [\mathbf{d}_2] \end{Bmatrix} \tag{21}$$

where $\mathbf{A_1}$, $\mathbf{A_2}$, $\mathbf{d}_1$, and $\dot{\mathbf{y}}_1$ correspond to the equations for the ship DOF, and $\mathbf{A}_3$, $\mathbf{A}_4$, $\mathbf{d}_2$, and $\dot{\mathbf{y}}_2$ correspond to the equations of the inverted pendulum DOF. This allows the dynamic problem to be solved using the lower partition:

$$\begin{bmatrix} & & \\ & \mathbf{A}_4 & \\ & & \end{bmatrix} \begin{Bmatrix} \\ \dot{\mathbf{y}}_2 \\ \end{Bmatrix} = \begin{Bmatrix} \\ \mathbf{d}_2 \\ \end{Bmatrix} - \begin{bmatrix} \\ \mathbf{A}_3 \\ \end{bmatrix} \begin{Bmatrix} \dot{\mathbf{y}}_1 \end{Bmatrix} \tag{22}$$

This is convenient because $\mathbf{A_1}$ contains the mass properties of the ship, and $\mathbf{d}_1$ contains the external forces acting on the ship, both of which are unknown. However, if the ship inertial properties were known, the applied forces could be determined, should they be of interest. Further, it is observed that the fully-coupled nature of the equations is retained such that the effect of the inverted pendulum on the ship, though small in practice, is not neglected.

4.3.1. Ship-Pendulum Reaction Forces

The translational DOF are defined such that they represent the accelerations of the ship in the ship frame rather than the inertial frame. They are modelled this way because the ship acceleration data, that will be used with the model, was recorded in the ship frame with an inertial sensor located near the point of interest. This avoids the need to transform the data to the point of interest which would require knowledge of the location of the centre of gravity of the ship which is not generally known, and is not constant due to consumption of fuel, potable water, stores, and active stabilization systems (when present and engaged).

It is useful to be able to solve for the translational reaction forces between the ship and the inverted pendulum. By adding new unknown force terms to the corresponding equations that were removed in the previous section, one can rearrange the equations to solve for the reaction forces while still including the prescribed ship accelerations.

If Eq. (22) is expanded to display the removed matrices and separate linear force terms, and $\mathbf{A}$ is instead partitioned into 18x3 submatrices it would appear as:

$$\begin{bmatrix} \mathbf{A}_1 & \mathbf{A}_2 & \mathbf{A}_3 & \mathbf{A}_4 & \mathbf{A}_5 & \mathbf{A}_6 \end{bmatrix} \begin{Bmatrix} \dot{\mathbf{y}}_1^1 \\ \dot{\mathbf{y}}_1^{1s} \\ \dot{\mathbf{y}}_2 \end{Bmatrix} = \begin{Bmatrix} \mathbf{d}_1 \\ \mathbf{d}_2 \end{Bmatrix} - \begin{bmatrix} \mathbf{A}_1 & \mathbf{A}_2 \end{bmatrix} \begin{Bmatrix} \dot{\mathbf{y}}_1^1 \\ \dot{\mathbf{y}}_1^{1s} \end{Bmatrix} + \begin{bmatrix} \\ \mathbf{V}_Q^{1s} \\ \end{bmatrix} \begin{Bmatrix} \mathbf{f}^{1s} \end{Bmatrix} \tag{23}$$

The greyed out terms are the ones that were transfered to the right side of the equation. When the forces are brought over to the left side of the equation and the ship angular terms removed, it becomes:

$$\begin{bmatrix} -\mathbf{V}_Q^{1s} & \mathbf{A}_3 & \mathbf{A}_4 & \mathbf{A}_5 & \mathbf{A}_6 \end{bmatrix} \begin{Bmatrix} \mathbf{f}^{1s} \\ \dot{\mathbf{y}}_2 \end{Bmatrix} = \begin{Bmatrix} \mathbf{d}_1 \\ \mathbf{d}_2 \end{Bmatrix} - \begin{bmatrix} \mathbf{A}_1 & \mathbf{A}_2 \end{bmatrix} \begin{Bmatrix} \dot{\mathbf{y}}_1^1 \\ \dot{\mathbf{y}}_1^{1s} \end{Bmatrix} \tag{24}$$

In this form the translational reaction forces can be solved for using the same mathematical procedure used to solve for the angular accelerations.

4.4. Method Used to Constrain Joints

In order to temporarily simplify the model to compare it to other models it is useful to be able to lock the DOF of the inverted pendulum. This can be done by simply removing any control forces, setting the positions and speeds of those DOF to zero at each time step, and removing the acceleration terms from the equations of motion. Furthermore, the equations for those DOF can be easily modified to solve for joint reaction forces and moments instead of the accelerations. Since relative angular velocity components between bodies are used as generalized speeds, then the constraining moment components will appear uncoupled in the corresponding equations [14]. For example, all of the joints can be locked and reaction moments solved for in Eq. (24) by setting all of the $\dot{\mathbf{y}}$ terms to zero and substituting with terms that allow one to solve for the reaction moments instead. The result with substitutions on the left hand side of the equation is:

$$\begin{bmatrix} \begin{bmatrix} -\mathbf{V}_Q^{1s} \end{bmatrix} \begin{bmatrix} -\mathbf{W}^1 \end{bmatrix} \begin{bmatrix} -\mathbf{W}^2 \end{bmatrix} \begin{bmatrix} -\mathbf{W}^3 \end{bmatrix} \begin{bmatrix} -\mathbf{W}^4 \end{bmatrix} \end{bmatrix} \begin{Bmatrix} \mathbf{f}^{1s} \\ \mathbf{m}^2 \\ \mathbf{m}^3 \\ \mathbf{m}^4 \\ \mathbf{m}^5 \end{Bmatrix} = \begin{Bmatrix} \mathbf{d} \end{Bmatrix} - \begin{bmatrix} \begin{bmatrix} \mathbf{A}_1 \end{bmatrix} \begin{bmatrix} \mathbf{A}_2 \end{bmatrix} \end{bmatrix} \begin{Bmatrix} \dot{\mathbf{y}}^1 \\ \dot{\mathbf{y}}^{1s} \end{Bmatrix} \tag{25}$$

4.5. Numerical Solution

As it was shown with Eq. (13) and the subsequent sections which derived its components, the equations of motion can be written as:

$$\mathbf{A}(\boldsymbol{\theta})\ddot{\mathbf{x}} + \mathbf{B}(\boldsymbol{\theta})\dot{\mathbf{x}} + \mathbf{C}(\boldsymbol{\theta}, \dot{\mathbf{x}})\dot{\mathbf{x}} = \boldsymbol{f}(\boldsymbol{\theta}) \tag{26}$$

which indicates that all of $\mathbf{A}$, $\mathbf{B}$, $\mathbf{C}$, and $\boldsymbol{f}$ are functions of the current state and therefore must be recalculated at each time step of the simulation. When performing a simulation using this equation the only unknown is $\ddot{\mathbf{x}}$ so the equation can be rearranged as:

$$\ddot{\mathbf{x}} = \mathbf{A}^{-1}(\boldsymbol{f} - \mathbf{B}\dot{\mathbf{x}} - \mathbf{C}\dot{\mathbf{x}}) \tag{27}$$

In order to use this equation with a time integration algorithm it is necessary to reduce it in order from N second order differential equations to $2N$ first order differential equations. One approach is to write,

$$\begin{bmatrix} \dot{\boldsymbol{\theta}} \\ \ddot{\mathbf{x}} \end{bmatrix} = \begin{bmatrix} \mathbf{T}\dot{\mathbf{x}} \\ \mathbf{A}^{-1}(\boldsymbol{f} - \mathbf{B}\dot{\mathbf{x}} - \mathbf{C}\dot{\mathbf{x}}) \end{bmatrix} \tag{28}$$

where the $\mathbf{T}$ is the transformation from generalized coordinate derivatives, $\dot{\mathbf{x}}$, to Bryant angle derivatives, $\dot{\boldsymbol{\theta}}$. These equations are numerically integrated to calculate updated values of $\dot{\mathbf{x}}$ and $\boldsymbol{\theta}$ at each time step.

5. MODEL VALIDATION

In order to validate the MATLAB code that simulates the dynamic equations of the four-link inverted pendulum model (4BAR), its simulation results were compared with three existing, published models that were created by members of the Carleton University Applied Dynamics Laboratory. The models were assigned the same mass properties and exposed to the same ship motions and control forces, and their states and reaction forces were compared.

The first model, GRM3D, was equivalent to having all four inverted pendulum joints constrained. The second model, PSM3D, was equivalent to having all but the first joint constrained. Input ship motions for these validations were obtained from two sources. The first was simulated ship data that was used to validate GRM3D against PSM3D. The second was actual ship motion data recorded during a recent heavy-weather sea trial aboard the Quest research vessel [15, 16] using an inertial sensor. The third model was equivalent to having no joints constrained, but input ship motion was limited to 1 DOF translational accelerations.

5.1. Comparison Metric

The metric used to compare the simulation results between models is called a normalized root mean square error (NRMSE) and is defined as:

$$NRMSE\ (\%) = \frac{\sqrt{\frac{1}{n}\sum(x_i^1 - x_i^2)^2}}{x_{max} - x_{min}} \times 100 \tag{29}$$

where x_i^1 and x_i^2 are data points from the first and second data sets, and n is the number of data points. Root mean square error is a useful metric for evaluation of the differences between datasets when the data are cyclic. With standard error calculations, normalized error calculations become inflated when both data sets approach zero which is less of an issue with root mean square calculations.

5.2. Validation with GRM3D

Graham's model is a 2D rigid body with no DOF attached to a ship base with 1 DOF of angular motion and 2 DOF of translational motion intended for studying human reactions to ship motion [17]. GRM3D is a spatial version of Graham's model that can be simulated in FORTRAN under any 6 DOF input deck motions and with various options for attachments to a hanging pendulum or a cart load [18]. If all of the joints in the 4BAR model are locked as formulated in Eq. (25), then it should behave the same as GRM3D, which provides an opportunity for model validation.

The simulated ship motion included velocities, accelerations, angular orientations, angular velocities, and angular accelerations. Reaction forces and moments were compared between the two models and the results are shown in Figs. 3 and 4.

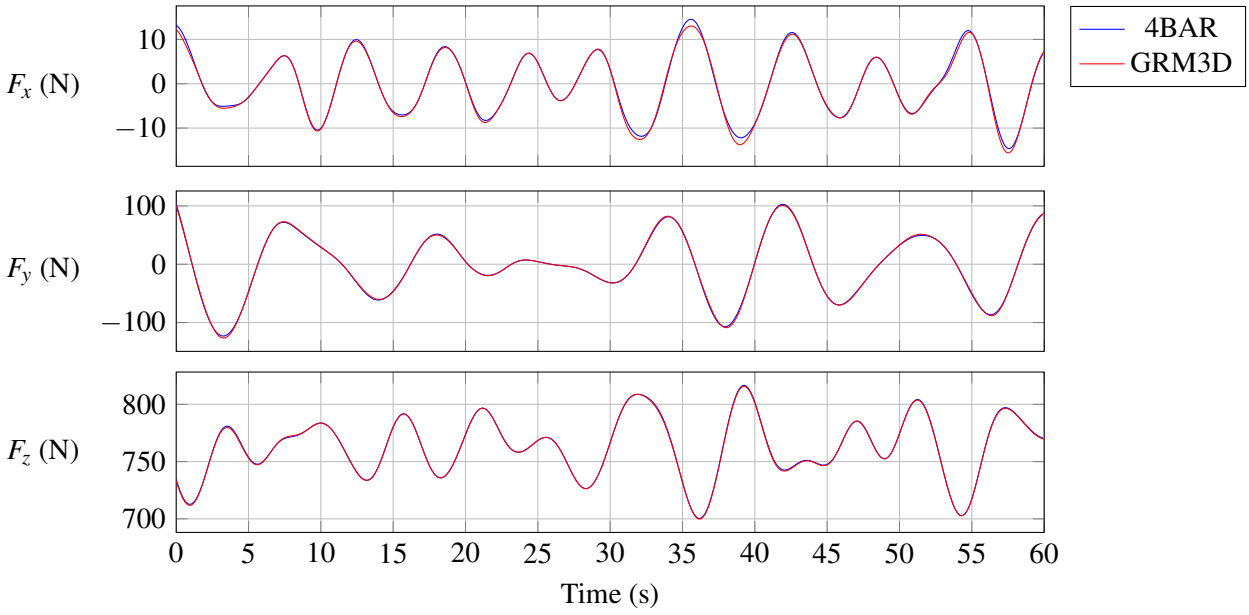

Fig. 3. Comparison of reaction forces between 4BAR and GRM3D. NRMSE 0.51% (F_x), 0.18% (F_y), and 0.15% (F_z).

5.3. Validation with PSM3D

PSM3D is a single-segment, single–joint spatial inverted pendulum postural stability model written in FORTRAN [5]. Similar to GRM3D, it can also be simulated under any prescribed motions and has various options for attachments to other rigid bodies and loadings. If all of 4BAR's joints are locked except for the

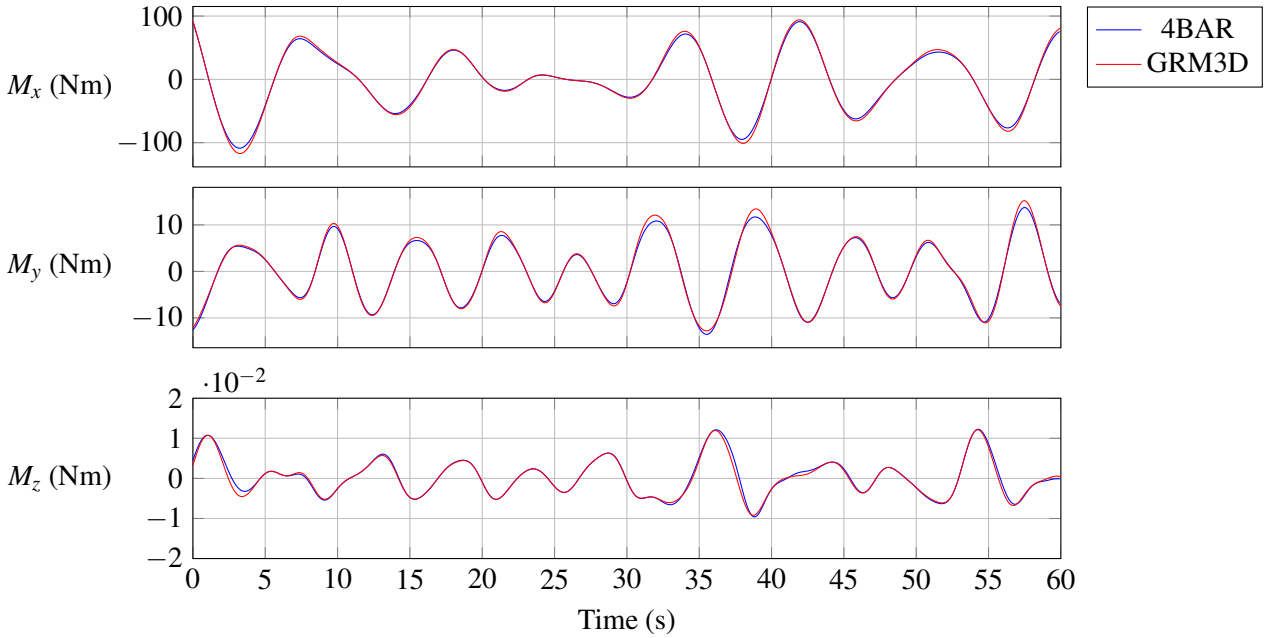

Fig. 4. Comparison of reaction moments between 4BAR and GRM3D. NRMSE 0.41% (M_x), 0.57% (M_y), and 0.80% (M_z).

first one, then it should behave the same as the PSM3D inverted pendulum model as long as both models use the same control system. In the PSM3D model there are control moments calculated for roll and pitch using a simple PD controller, which was implemented in the 4BAR model.

Four primary validation tests were run for the two models. The first used the same generated ship motion that was used for the GRM3D comparison. The second and third used two different six-minute recordings of measured ship motion. The fourth used a forty-minute recording from the same sensor. The results from all four tests were equally successful, and graphed results from the second test are shown in Figs. 5 and 6.

5.4. Validation of Multiple Links

For validation of the model with no joints constrained there was not a spatial model readily available, so instead, a comparison was made with a published 2D cart–inverted pendulum model [19]. The equations of motion used for the cart–inverted pendulum model (CARTIP) were:

$$\mathbf{M}\ddot{\mathbf{q}} + \mathbf{C}\dot{\mathbf{q}} + \mathbf{K}\mathbf{q} = 0 \tag{30}$$

where **M**, **K**, and **C** are the mass, stiffness, and damping matrices.

In 2D, the only difference between the cart–inverted pendulum model and the ship-inverted pendulum model is that the ship can experience rotational motion as well as translational motion. For this test, the input ship motion was reduced to one degree of freedom translational motion.

The results of the test are shown in Fig 7. The data shown is for the fourth link, because its motions and errors were the largest. The other links all had very similar results.

6. CONCLUSIONS

Comparisons of the new spatial inverted pendulum model with existing models show that the new model performs almost exactly the same as existing ones. The small differences between models are attributed to

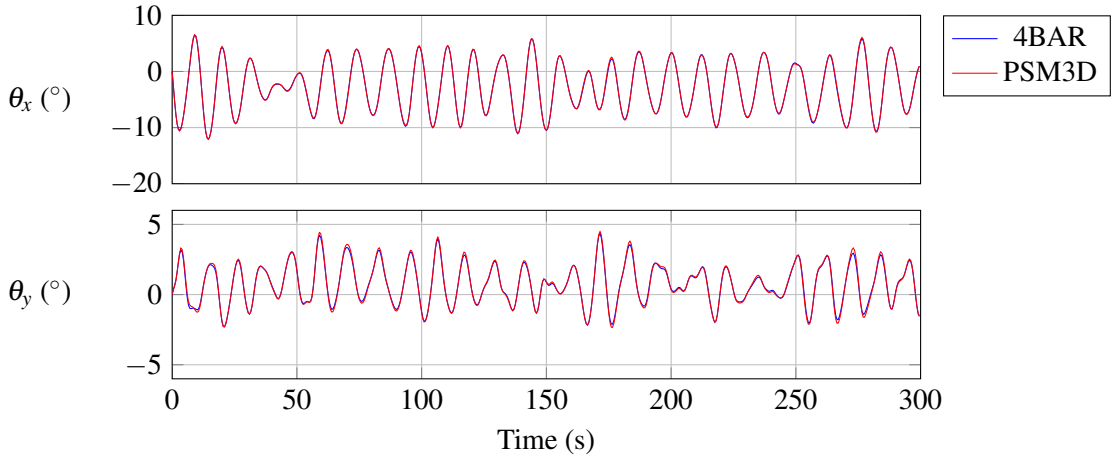

Fig. 5. Validation test angles for 4BAR and PSM3D. NRMSE 0.32% (θ_x) and 0.45% (θ_y).

variations in implementation resulting in computational differences between the MATLAB and FORTRAN models. Future work on the derived model will involve developing a control system which combines experimental sensory data with the complexity of a four-link spatial model, which will be used to better understand human postural stability control strategies.

REFERENCES

1. Schiehlen, W. "Multibody system dynamics: roots and perspectives." *Multibody System Dynamics*, Vol. 1, No. 2, pp. 149–188, 1997.
2. Langlois, R. and Anderson, R. "Multibody dynamics of very flexible damped systems." *Multibody System Dynamics*, Vol. 3(2), pp. 109–136, May 1999.
3. Sovol, A., Bustamante Valles, K., Riedel, S. and Harris, G. "Bi-planar postural stability model: Fitting model parameters to patient data automatically." In "32nd Annual International Conference of the IEEE IMBS," Buenos Aires, Argentina, 2010.
4. Wedge, J. and Langlois, R. "Simulating the effects of ship motion on postural stability using articulated dynamic models." In "2003 Summer Computer Simulation Conference," The Society for Modeling and Simulation International, Montreal, Canada, 2003.
5. Langlois, R.G. "Development of a spatial inverted pendulum shipboard postural stability model." In "International Conference on Human Performance at Sea," Glasgow, Scotland, UK, 2010.
6. Xinjilefu, X., Hayward, V. and Michalska, H. "Stabilization of the spatial double inverted pendulum using stochastic programming seen as a model of standing postural control." In "9th IEEE-RAS International Conference on Humanoid Robots," Paris, France, 2009.
7. Stockwell, C., Koozekanai, S. and Barin, K. "A physical model of human postural dynamics." *Annals of the New York Academy of Sciences*, Vol. 374, pp. 722–730, 1981.
8. Barin, K. "Evaluation of a generalized model of human postural dynamics and control in the sagittal plane." *Journal of Biological Cybernetics*, Vol. 61, pp. 37–50, 1989.
9. Kuo, A. and Zajac, F. "Human standing posture: Multijoint movement strategies based on biomechanical constraints." *Progress in Brain Research*, Vol. 97, pp. 349–358, 1993.
10. Diener, H.C., Dichgans, J., Bruzek, W. and Selinka, H. "Stabilization of human posture during induced oscillations of the body." *Experimental Brain Research*, Vol. 45, pp. 126–132, 1982.
11. Bos, J. "Feasibility of motion induced interruption (MII) prediction." Tech. Rep., TNO Human Factors Research Institute, 1999.
12. Maki, B., McIlroy, W. and Perry, S. "Influence of lateral destabilization on compensatory stepping responses." *Journal of Biomechanics*, Vol. 29(3), pp. 343–353, 1996.

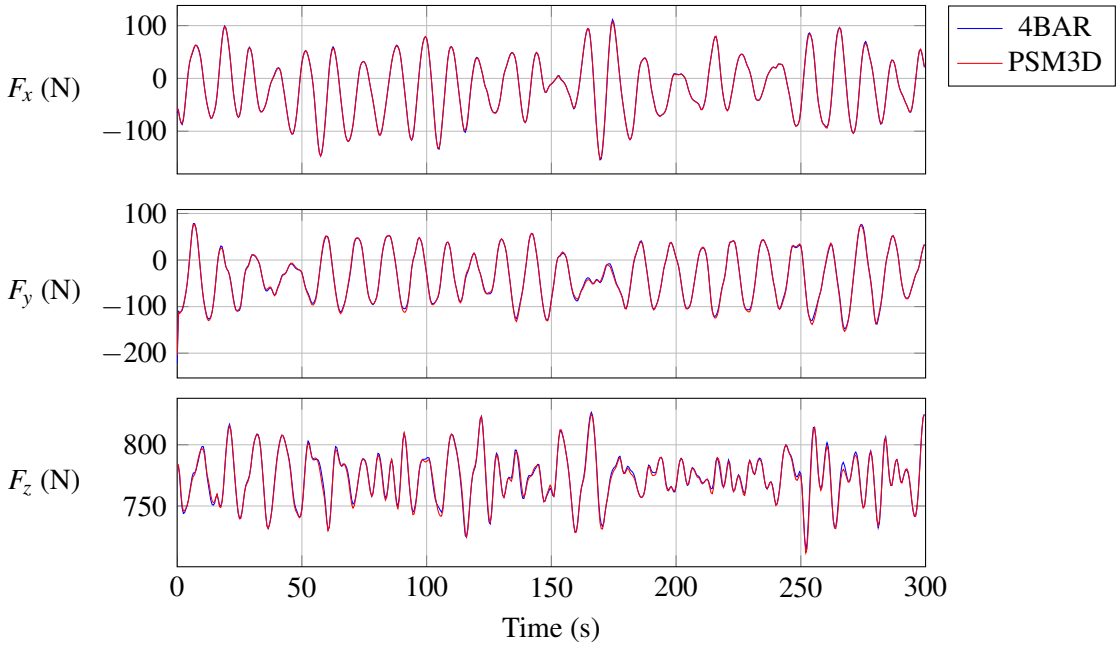

Fig. 6. Validation test reaction forces for 4BAR and PSM3D. NRMSE 0.51% (F_x), 0.85% (F_y), and 1.61% (F_z).

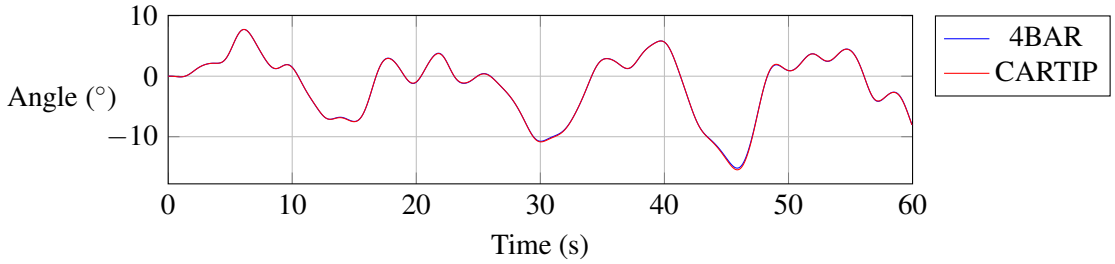

Fig. 7. Multi-link validation test results for fourth link. NRMSE values range from 0.1658 % to 0.2922 %.

13. Amirouche, F. *Fundamentals of Multibody Dynamics*. Birkhauser Boston, 2006.
14. Huston, R. *Multibody Dynamics*. Butterworth-Heinemann, 1990.
15. Bourgeois, N., Langlois, R. and Hunter, A. "Quest Q-348 sea trial: Human postural stability studies." In "International Conference of Control, Dynamic Systems, and Robotics," Ottawa, Canada, 2014.
16. Hunter, A., Bourgeois, N. and Langlois, R. "The impact of motion induced interruptions on cognitive performance." In "International Conference on Applied Human Factors and Ergonomics," Poland, 2014.
17. Graham, R., Baitis, A. and Meyers, W. "On the development of seakeeping criteria." *Naval Engineers Journal*, Vol. 104, pp. 259–275, 1992.
18. Morris, H. and Langlois, R. "Generic stance geometry model for determining postural stability motion induced interruption onsets." In "International Conference of Control, Dynamic Systems, and Robotics," Ottawa, Canada, 2014.
19. Langlois, R. and Anderson, R. "A tutorial presentation of alternative solutions to the flexible beam on rigid cart problem." In "Transactions of the Canadian Society for Mechanical Engineering," Vol. 29, pp. 357–373, 2005.